Ajay Singh
Editor

Emergency Radiology

Imaging of Acute Pathologies

Springer

Ajay Singh
Editor

Emergency Radiology

Imaging of Acute Pathologies

Springer

Editor
Ajay Singh, MD
Department of Radiology
Massachusetts General Hospital
Harvard Medical School
Boston, MA
USA

ISBN 978-1-4419-9591-9 ISBN 978-1-4419-9592-6 (eBook)
DOI 10.1007/978-1-4419-9592-6
Springer New York Heidelberg Dordrecht London

Library of Congress Control Number: 2013938161

Printed on acid-free paper

Springer is part of Springer Science+Business Media (www.springer.com)

Preface

The practice of emergency radiology has evolved rapidly over the last two decades, playing an important part in the triage of emergency room patients. Plain radiography and CT imaging are the most commonly used imaging modalities in managing emergency conditions in the more than 115,000 patients visiting the emergency room. Ultrasound, MR, and nuclear medicine imaging, although less often used, play crucial roles in managing specific conditions.

This textbook of emergency radiology represents the state-of-the-art radiology practice in the management of emergency room patients by leading experts in the field. The chapters are based on different organ systems, with few chapters being imaging modality based.

I would like to take this opportunity to thank the publishers for the privilege of editing this textbook and their staff for professional production of this issue. I must thank the authors of the book chapters for sharing their expertise and case material in preparing the manuscript.

Boston, MA, USA

Ajay Singh, MD

Contents

Contributors

Laura Avery, MD Department of Radiology, Massachusetts General Hospital, Boston, MA, USA

Brett W. Carter, MD Department of Radiology, Baylor University Medical Center, Dallas, TX, USA

Harigovinda R. Challa, MD Division of Pediatric Radiology, University of Kentucky, Lexington, KY, USA

Andrew Chen, MD Department of Radiology, University of Massachusetts, Worcester, MA, USA

Jeanette Chun, MD Department of Radiology, University of Massachusetts Memorial Medical Center, Worcester, MA, USA

Dennis Coughlin, MD Department of Radiology, University of Massachusetts Memorial Medical Center, Worcester, MA, USA

Terry S. Desser, MD Department of Radiology, Stanford University School of Medicine, Stanford, CA, USA

Johanne E. Dillon, MD Division of Pediatric Radiology, University of Kentucky, Lexington, KY, USA

Sathish Kumar Dundamadappa, MD Department of Radiology, University of Massachusetts, Worcester, MA, USA

Melanie Ehinger, MD Department of Radiology, University of Massachusetts, Worcester, MA, USA

Joseph Ferucci, MD Department of Radiology, University of Massachusetts Memorial Medical Center, Worcester, MA, USA

Dale E. Hansen III, MD Department of Radiology, University of Tennessee, Memphis, TN, USA

Chris Heinis, MD Department of Emergency Radiology, University of Massachusetts Memorial Medical Center, Worcester, MA, USA

Paul F. von Herrmann, MD Department of Radiology, University of Kentucky, Lexington, KY, USA

Mai-Lan Ho, MD Department of Radiology, Beth Israel Deaconess Medical Center, Boston, MA, USA

Paul Jaffray, MD Department of Radiology, University of Massachusetts Memorial Medical Center, Worcester, MA, USA

Rathachai Kaewlai, MD Department of Radiology, Ramathibodi Hospital and Mahidol University, Ratchatewi, Bangkok, Thailand

Majid Khan, MD Department of Radiology, Oakland University, William Beaumont School of Medicine, William Beaumont Hospital, Royal Oak, MI, USA

Amisha Khicha, MD Department of Radiology, Wesley Medical Center, University of Kansas School of Medicine, Wichita, KS, USA

John J. Krol, MD Department of Radiology, University of Kentucky, Lexington, KY, USA

Joshua Leeman, MD Department of Radiology, Shady Side Hospital, Pittsburgh, PA, USA

Jonathan E. Leeman, MD Department of Radiology, Shady Side Hospital, Pittsburgh, PA, USA

Robin Levenson, MD Department of Radiology, Beth Israel Deaconess Medical Center, Boston, MA, USA

Chris Malcom, MD Department of Radiology, William Beaumont Hospital, Royal Oak, MI, USA

Caterina Missiroli, MD Department of Diagnostic Imaging, Azienda Ospedaliera della Provincia di Lecco – Presidio Ospedaliero A. Manzoni, Lecco, Italy

Victorine V. Muse, MD Department of Radiology, Massachusetts General Hospital, Harvard Medical School, Boston, MA, USA

David J. Nickels, MD, MBA Department of Radiology, Division of Emergency Radiology, University of Kentucky, Lexington, KY, USA

Robert A. Novelline, MD Department of Radiology, Massachusetts General Hospital, Harvard Medical School, Boston, MA, USA

M. Elizabeth Oates, MD Department of Radiology, University of Kentucky, Lexington, KY, USA

Neil Patel, MD Department of Radiology, University of Tennessee, Memphis, TN, USA

Sneha Patel, MD Department of Diagnostic Radiology, William Beaumont Hospital, Royal Oak, MI, USA

Parul Penkar, MD Department of Radiology, Massachusetts General Hospital, Boston, MA, USA

Sridhar Shankar, MD, MBA Department of Radiology, University of Tennessee, Memphis, TN, USA

Ajay Singh, MD Department of Radiology, Massachusetts General Hospital, Harvard Medical School, Boston, MA, USA

Benjamin Yeh, MD Department of Radiology, University of California San Francisco, San Francisco, CA, USA

Imaging of Acute Aortic Conditions

1

Jeanette Chun and Ajay Singh

Introduction

Acute aortic conditions include, but are not limited to, aortic rupture, aortic dissection, intramural hematoma, and penetrating aortic ulcer. Prompt diagnosis of these conditions is essential for managing these conditions. Because these conditions often have similar symptoms, namely, chest and abdominal pain, the imaging characteristics are key to prompt and accurate diagnosis.

Abdominal Aortic Aneurysm and Aortic Rupture

Abdominal aortic aneurysm (AAA) is seen in 5–10 % of elderly male smokers. Most AAAs are true aneurysms and involve all three layers of the aortic wall. The two most common etiologies of AAA are degenerative and inflammatory (Table 1.1).

Other less frequent etiologies of AAA include mycotic aneurysm, which constitutes 1–3 % of aortic aneurysms. However, mycotic aneurysm is known to more commonly involve aorta than any other artery. Staphylococcus and Streptococcus species are the most common pathogens of mycotic aneurysm. The cases of mycotic aneurysm due to Salmonella species are more common in East Asia and demonstrate an early tendency to rupture.

The most significant complication of AAA is aortic rupture. The mortality rate for ruptured AAA is 50 %; thus, an accurate diagnosis is essential for prompt surgical intervention. The risk of rupture is proportional to the maximum cross-sectional diameter, with 1 %/year risk for aneurysms measuring 5–5.9 cm. The risk of rupture increases up to 20 %/year for an aneurysm measuring greater than 7 cm in diameter. Although AAAs are less common in females (M:F = 4:1), they are more likely to rupture when compared to males.

Table 1.1 Causes of abdominal aortic aneurysm

Degenerative (most common)
Inflammatory (5–10 % of all)
Mycotic
Syndromes: Marfan's syndrome, Ehlers-Danlos syndrome
Vasculitis: Takayasu's disease, Behcet's disease
Traumatic

Ultrasound is the most commonly used imaging modality to screen for AAA and has been shown to reduce mortality. The imaging criteria to diagnose AAA include aortic caliber of more than 3 cm and an aortic caliber of more than 1.5 times the expected diameter of the abdominal aorta (Fig. 1.1). The aortic caliber is measured perpendicular to the long axis of the aorta, from outer wall to outer wall. Although ultrasound is highly sensitive in making the diagnosis of abdominal aortic aneurysm, it is not as reliable as CT in diagnosing aortic rupture. However, the demonstration of normal caliber of abdominal aorta by ultrasound makes aortic rupture an unlikely possibility.

Most aortic aneurysms rupture involves the middle third of the aneurysm, through the posterolateral wall and into the retroperitoneum (Fig. 1.2a). However, intraperitoneal rupture and rupture into the bowel (usually the duodenum) and very rarely into the IVC may occur (Fig. 1.2b, c).

Risk Factors for Aortic Rupture

Progressive aneurysmal dilatation of the aorta with increased wall tension is directly related to the risk of rupture. The

J. Chun, MD
Department of Radiology,
University of Massachusetts Memorial Medical Center,
Worcester, MA, USA

A. Singh, MD (✉)
Department of Radiology,
Massachusetts General Hospital, Harvard Medical School,
10 Museum Way, # 524, Boston, MA 02141, USA
e-mail: asingh1@partners.org

A. Singh (ed.), *Emergency Radiology*,
DOI 10.1007/978-1-4419-9592-6_1,

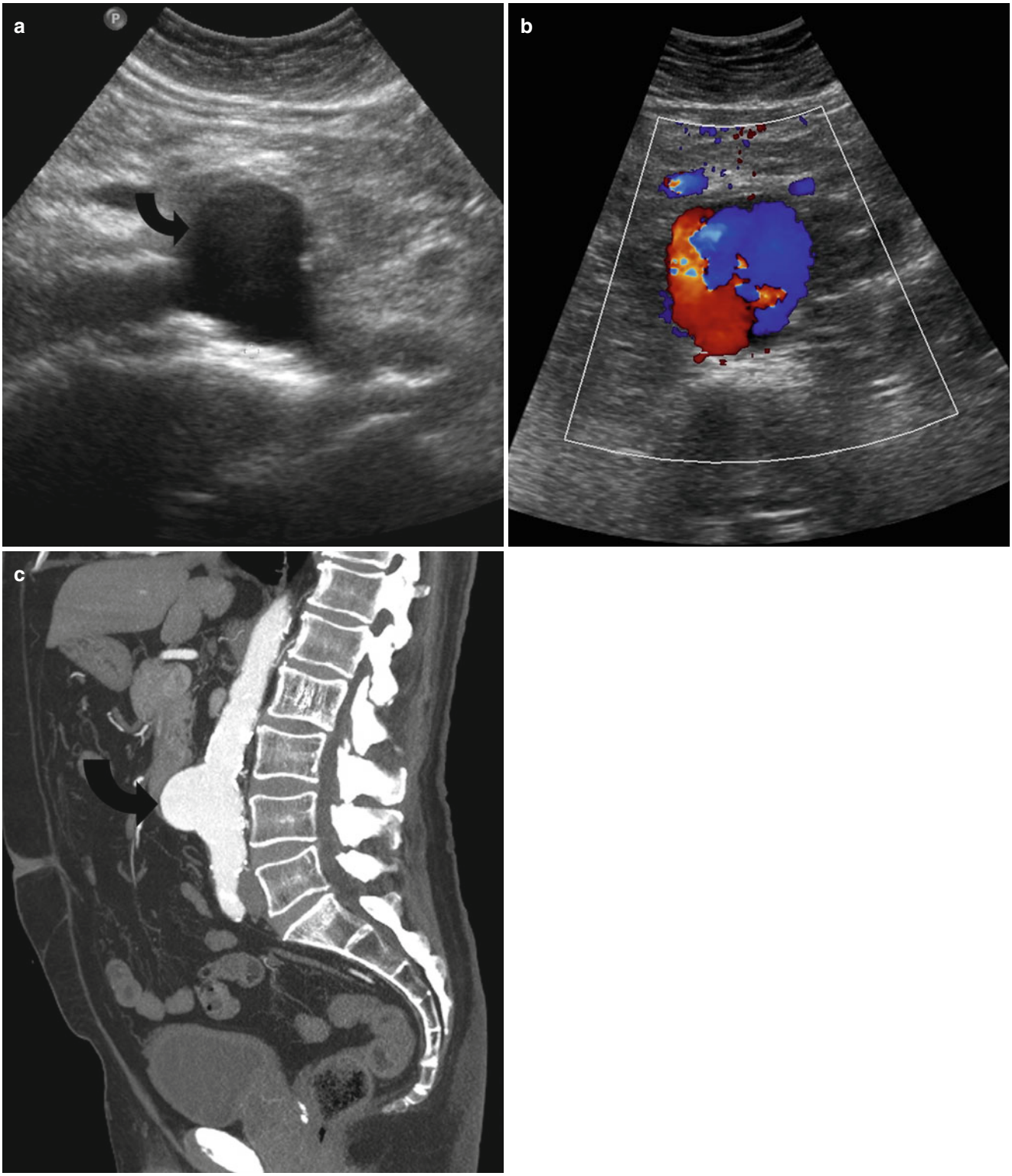

Fig. 1.1 Saccular abdominal aortic aneurysm. (**a** and **b**) US demonstrate a saccular infrarenal aortic aneurysm (*curved arrow*) with yin-yang sign on color Doppler imaging. (**c**) Sagittal reformation demonstrates the saccular infrarenal abdominal aortic aneurysm (*curved arrow*)

decreased proportion of thrombus to lumen ratio is also thought to play a part, as a larger thrombus better protects against rupture by providing protection against the high aortic pressures [1]. In addition, the amount of thrombus calcification, which is thought to be related to the amount of thrombus present, is also an indirect measure [2].

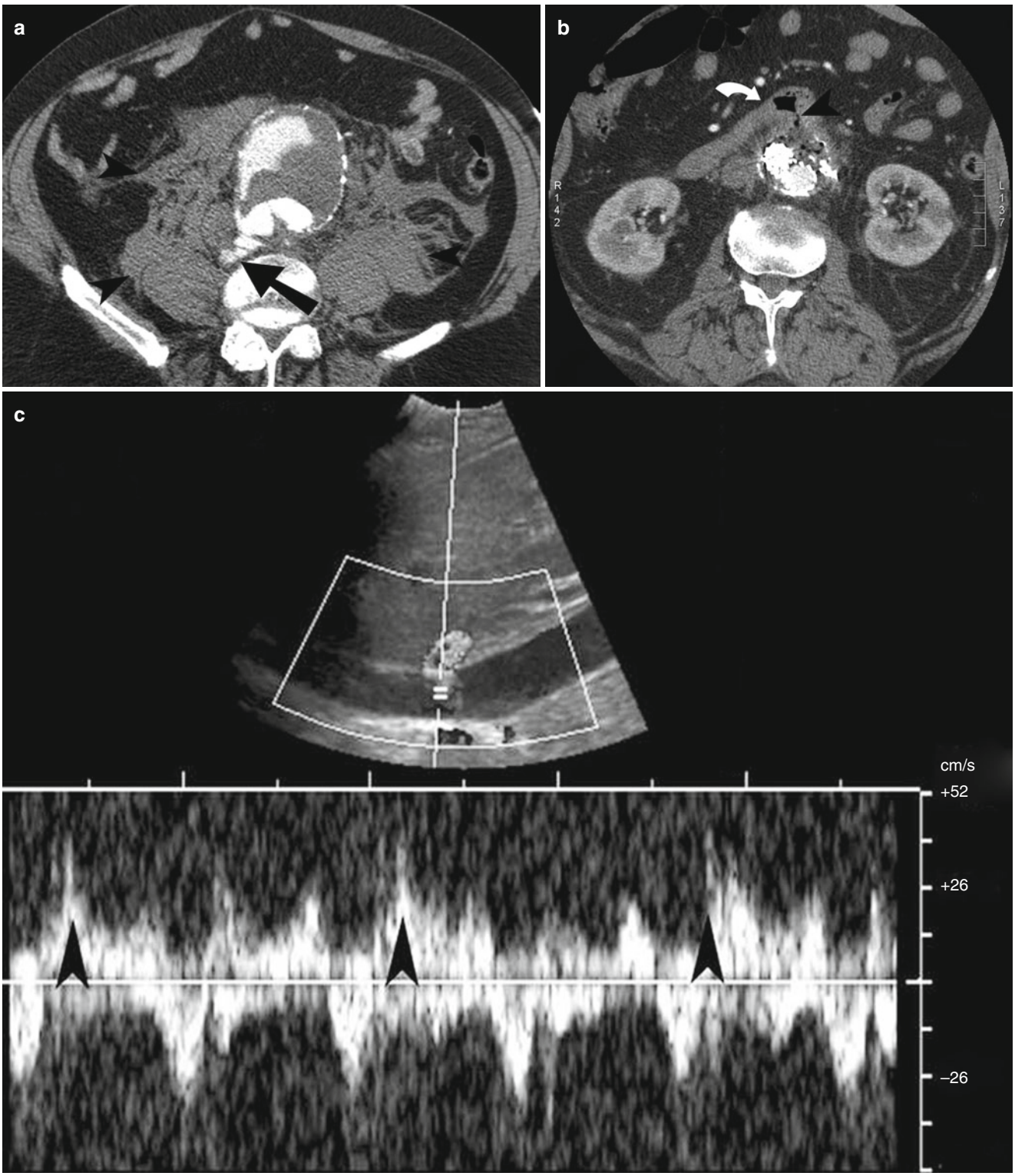

Fig. 1.2 Abdominal aortic aneurysm rupture, aorto-enteric and aorto-caval fistula. (**a**) Contrast-enhanced CT scan study of the lower abdomen demonstrates active extravasation of contrast (*arrow*) from infrarenal abdominal aortic aneurysm. There is retroperitoneal hemorrhage (*arrowheads*) identified around the aortic aneurysm. (**b**) Aorto-enteric fistula. Contrast-enhanced CT scan study demonstrates communication (*arrowhead*) of the third portion of the duodenum (*arrow*) with the infrarenal abdominal aortic aneurysm sac. The patient had recently undergone endovascular stent placement. (**c**) Aortocaval fistula. Doppler US shows the combination of arterial and venous spectral waveform in the inferior vena cava lumen, in a patient with aortocaval fistula

Table 1.2 CT findings of aortic rupture

1. Active extravasation of contrast
2. Retroperitoneal hematoma around the aortic aneurysm
3. Periaortic stranding
4. Draped aorta sign
5. Hyperdense crescent sign
6. Tangential calcium sign
7. Discontinuity of intimal calcification

Imaging

The imaging modality of choice is a contrast-enhanced multidetector CT (MDCT). The CT can demonstrate an AAA with surrounding retroperitoneal hemorrhage into psoas compartment, pararenal space, and perirenal space. A contrast-enhanced CT provides additional information about the aortic size, presence or absence of active extravasation, and anatomic relationships (Table 1.2). A hyperdense crescent sign and draped aorta sign are indicators of contained aortic leak or impending rupture. Focal discontinuity of intimal calcification is also a secondary sign of aortic rupture.

Hyperdense Crescent Sign

Hyperdense crescent sign is seen as a well-defined peripheral, high-density, crescent configuration within a thrombus where there is internal dissection of hemorrhage into the thrombus and ultimately reaching the aortic wall. It is a sign of acute or impending rupture (Fig. 1.3a) [1].

Draped Aorta Sign

Draped aorta sign indicates a contained aortic rupture and shows posterior aortic wall not identifiable as a separate structure and draping over the adjacent vertebral bodies (Fig. 1.3b, c). If rupture should occur, the most common sign of aneurysmal rupture is a retroperitoneal hematoma adjacent to the aneurysm.

Tangential Calcium Sign

The intimal calcification in the aorta points away from the circumference of the aneurysm (Fig. 1.3d).

The typical imaging features of mycotic aneurysm (Fig. 1.3e) include rapidly increasing caliber of a saccular aortic aneurysm with wall irregularity, periaortic edema and soft tissue mass, and the presence of gas. Periaortic soft tissue stranding and soft tissue mass are the most common features seen on imaging of mycotic aneurysm. Calcifications and thrombus are uncommon in a mycotic aneurysm. The lack of calcification in the aortic wall is due to the nonatherosclerotic origin of the aneurysm.

Aortic Dissection

Aortic dissection is the most common acute presentation involving the aorta [3]. It usually originates with a tear in the intima, which causes high-pressure blood to enter and dissect the aortic wall (Table 1.3).

The most commonly used classification for aortic dissection is the Stanford classification system.

1. *Type A aortic dissection:* Regardless of origin and extent of dissection, a Type A aortic dissection involves the ascending aorta (Fig. 1.4) [4]. The potential for complications with Type A dissection necessitates urgent surgical intervention [4]. The complications include dissection into the pericardium resulting in cardiac tamponade, dissection into the coronary arteries resulting in occlusion, and aortic insufficiency with involvement of the valve [4].
2. *Type B aortic dissection:* The aortic dissection originates past the left subclavian artery [5]. Unlike Type A dissection, the Type B dissections are usually medically treated.

Imaging

The imaging modality of choice to evaluate aortic dissection is MDCT. It allows accurate assessment of the extent of the disease, including the origin of the dissection, involvement of the visceral branches, and presence of a false lumen [3, 4]. The most characteristic findings of aortic dissection include an intimal flap and two distinct lumens. Secondary findings include intimal displacement of calcified wall, delayed enhancement of false lumen, pericardial or mediastinal hematoma, and ischemia or infarction of distal organs supplied by the false lumen [4].

True Versus False Lumen

Once the recognition of an aortic dissection is made, it is important to distinguish between the true and false lumen for treatment purposes, especially endovascular repair. Lepage et al. evaluated signs to distinguish between the true and false lumen and determined two consistent signs: beak sign and larger cross-sectional area of false lumen as the best indicators. The beak sign is present in the false lumen and consists of an acute angle between the dissection flap and the aortic wall [5]. The larger caliber lumen is generally the false lumen and is most commonly present anteriorly, to the right side in the ascending aorta (Figs. 1.4, 1.5, and 1.6). In the descending thoracic aorta, the false lumen is most

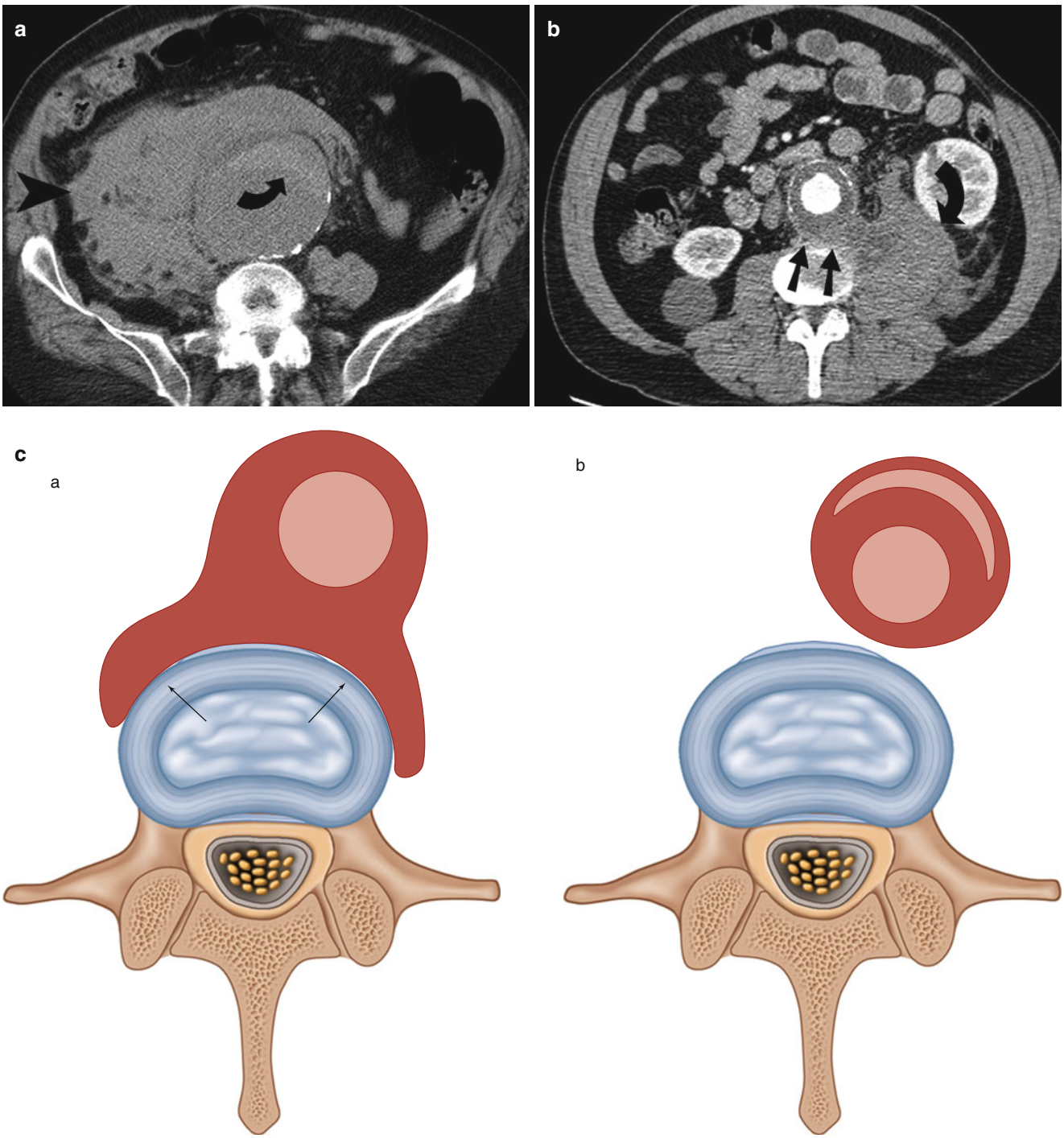

Fig. 1.3 CT features of abdominal aortic aneurysm rupture. (**a**) Hyperdense crescent sign. Noncontrast CT demonstrates large retroperitoneal hematoma (*arrowhead*) from the ruptured aortic aneurysm. A hyperdense crescent (*curved arrow*) is present in the anterior wall of the infrarenal abdominal aortic aneurysm. (**b**) Draped aorta sign. Contrast-enhanced CT demonstrates draping of the posterior wall of the aorta (*straight arrows*) on the anterior aspect of the lumbar spine. There is large retroperitoneal hematoma (*curved arrow*) identified in the psoas compartment and left posterior pararenal space. (**c**) Schematic representation of the *draped aorta sign* (*a*) and *hyperdense crescent sign* (*b*). Draped aorta sign is characterized by draping of deficient aortic wall on the anterior aspect of the vertebral body. Hyperdense crescent sign is characterized by the presence of a high-density sickle-shaped blood clot in the aortic wall. (**d**) Tangential calcium sign in a patient with contained aortic leak. Noncontrast CT demonstrates intimal calcifications (*arrowheads*) displaced from their expected location and pointing away from the aortic circumference. (**e**) Rupture of mycotic aneurysm. Noncontrast CT demonstrates air in the wall of the aortic aneurysm, secondary to clostridial infection. Breech in the aortic wall is indicated by the presence of air (*arrowheads*) outside the aortic adventitia

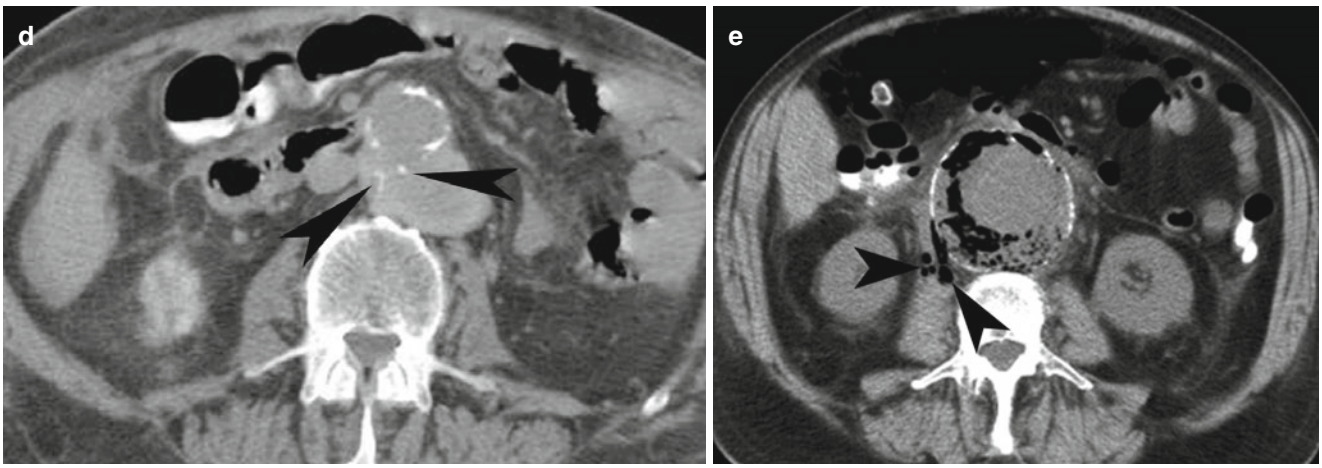

Fig. 1.3 (continued)

Table 1.3 Factors predisposing to aortic dissection

Hypertension (most common)
Syndromes
Marfan's syndrome
Turner syndrome
Noonan syndrome
Ehlers-Danlos syndrome
Coarctation, bicuspid aortic valve
Cocaine use
Pregnancy
Trauma

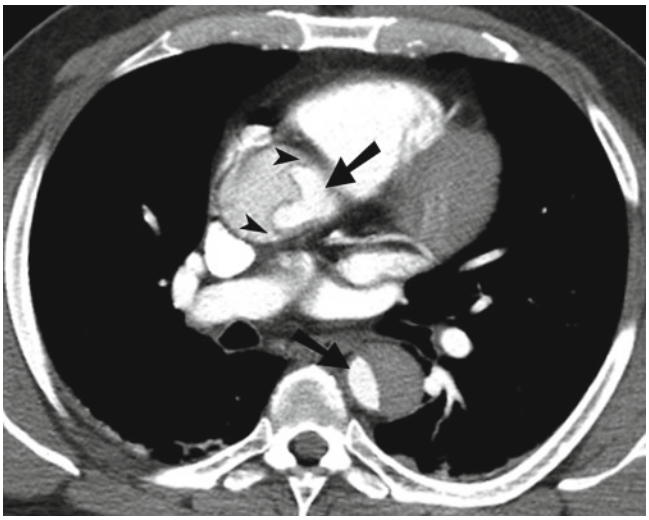

Fig. 1.4 Type A aortic dissection. Contrast-enhanced CT scan study of the chest demonstrates aortic dissection involving the ascending as well as the descending thoracic aorta. The true lumen can be identified by the smaller caliber (*arrows*) and higher density. The beak sign (*arrowheads*) is identified in the false lumen

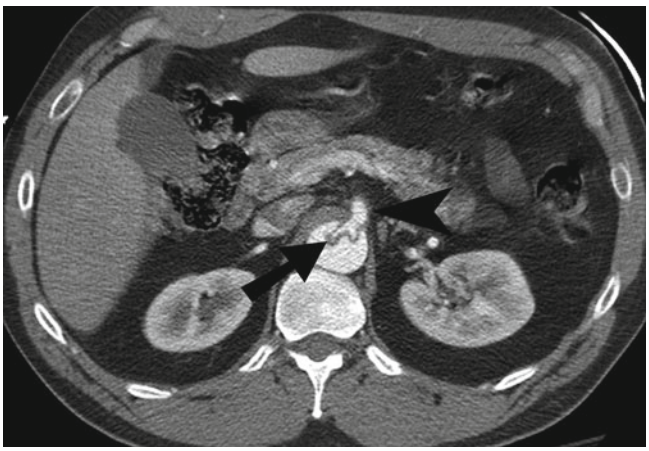

Fig. 1.5 Aortic dissection involving the abdominal aorta. Contrast-enhanced CT scan study demonstrates small caliber of the true lumen (*arrow*) supplying the superior mesenteric artery (*arrowhead*)

often seen posteriorly and to the left. Cobwebs are seen in the false lumen while aortic wall calcifications are usually seen around true lumen.

Intramural Hematoma

Intramural hematoma is a hematoma that has dissected through the media without an originating intimal tear (Figs. 1.7 and 1.8). The intramural hematoma may represent hemorrhage of the vasa vasorum (nutrient vessels for the vessel wall) that has dissected through the media [6]. It can be seen in hypertensive and can also be seen after blunt trauma. It can progress to rupture of the aortic wall or aortic dissection.

Fig. 1.6 Type B aortic dissection on MR angiogram. Gadolinium-enhanced MR angiogram demonstrates the dissection flap (*arrowheads*) present in the descending thoracic aorta

Unlike mural thrombus, intramural hematoma is deep to the intimal calcification and does not demonstrate the continuous flow seen with aortic dissection. Intramural hematoma can be diagnosed on CT, transesophageal echocardiography, and MRI. Since there is no intimal disruption, it cannot be diagnosed on conventional aortography. The treatment of intramural hematoma is similar to aortic dissection.

Penetrating Ulcer

Penetrating ulcer is characterized by atherosclerotic ulceration that has penetrated through the elastic lamina and formed a hematoma in the media. On CT scan, it is seen as an ulcer with focal hematoma and adjacent arterial wall thickening (Fig. 1.9) [7, 8]. Unlike penetrating ulcer, an atherosclerotic plaque with ulceration does not extend beyond the intima and is not associated with intramural hematoma.

Penetrating ulcer and aortic dissection are characterized by disruption of the intima, while aortic rupture is characterized by disruption of the aortic wall.

CT is the key diagnostic modality in the emergency room evaluation of acute aortic syndromes and allows different pathologies to be diagnosed for proper triage as well as treatment.

Teaching Points

- There is increased risk of rupture with increasing caliber of the aneurysm and reduced thrombus to lumen ratio.
- Hyperdense crescent sign and draped aorta sign are indicators of contained aortic leak or impending rupture.
- Type A aortic dissection involves the ascending aorta and is surgically managed.
- Type B aortic dissection originates past the left subclavian artery and is usually medically managed.
- Intramural hematoma represents hemorrhage of the vasa vasorum and is not associated with intimal discontinuity (unlike penetrating ulcer).

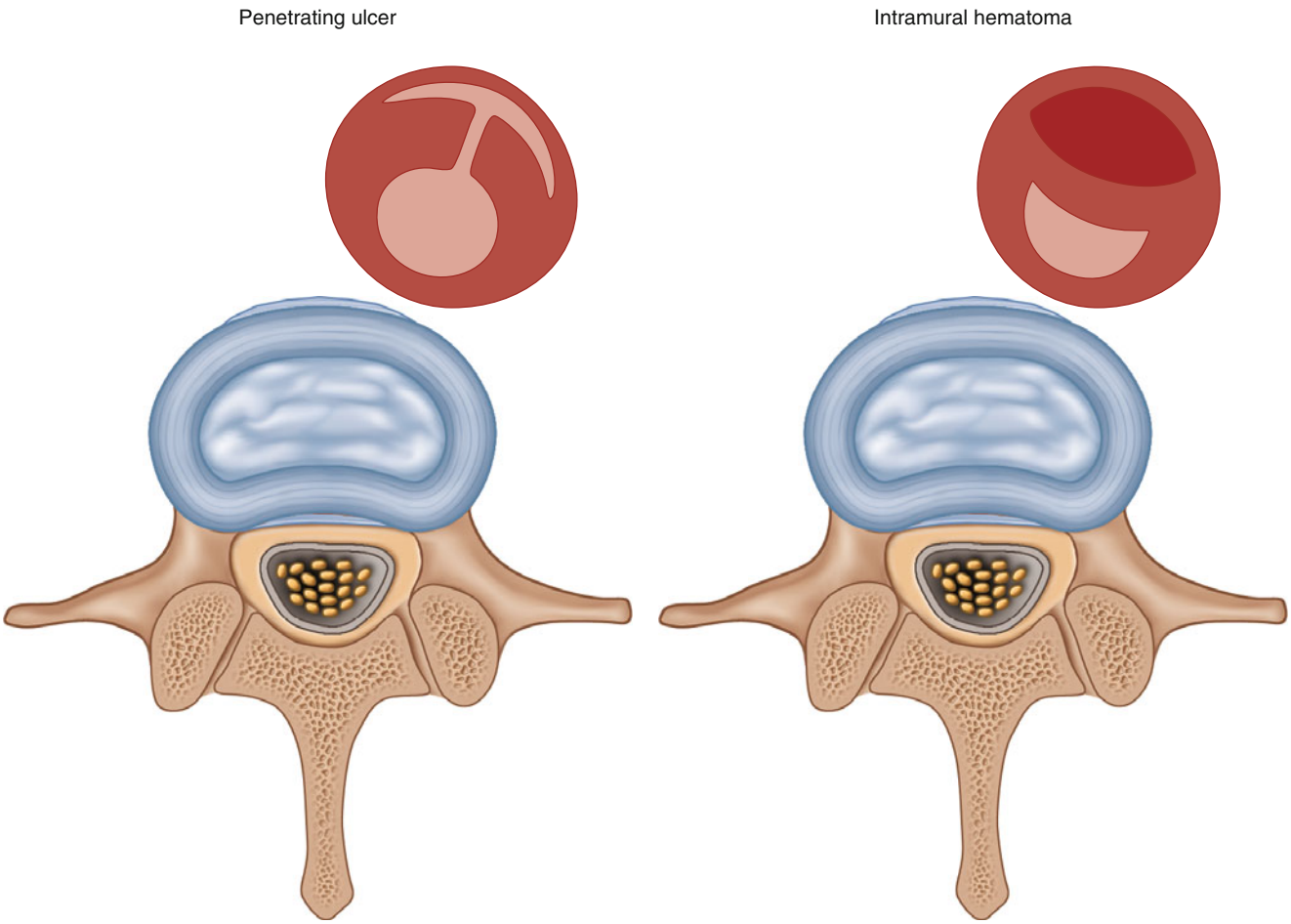

Fig. 1.7 Schematic representation of penetrating ulcer and intramural hematoma. Penetrating ulcer is characterized by communication of the arterial lumen with the hematoma located in the media. Intramural hematoma is characterized by lack of direct communication of the arterial lumen with the hematoma in the media

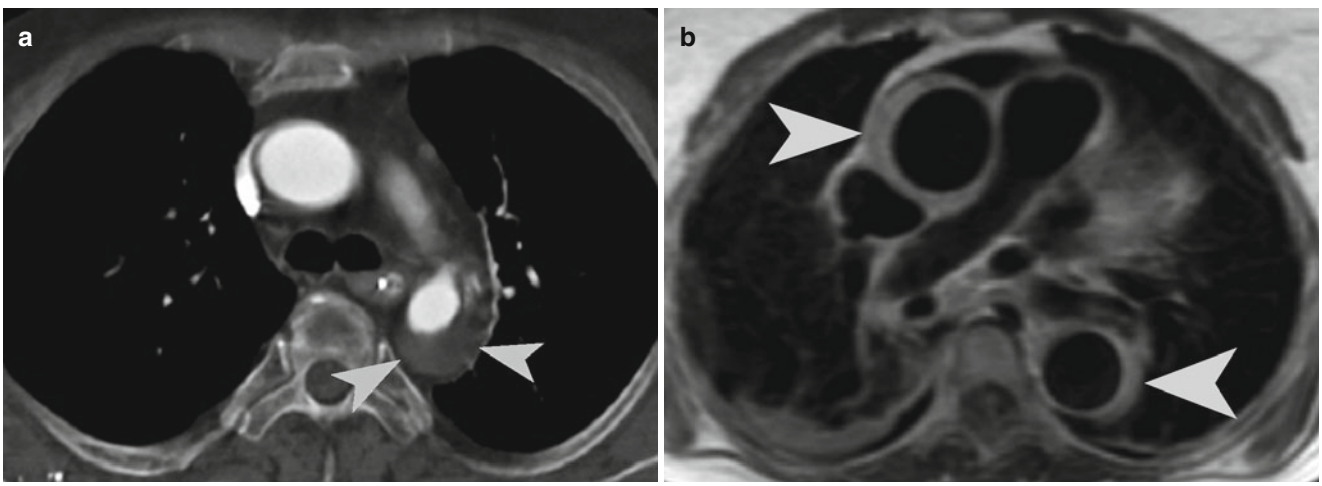

Fig. 1.8 Intramural hematoma. (**a**) Contrast-enhanced CT demonstrates asymmetric aortic wall thickening, consistent with intramural hematoma (*arrowheads*) in the descending thoracic aorta. (**b**) Noncontrast axial T1-weighted MR shows intramural hematoma (*arrowheads*) causing asymmetric aortic wall thickening in the ascending and descending thoracic aorta

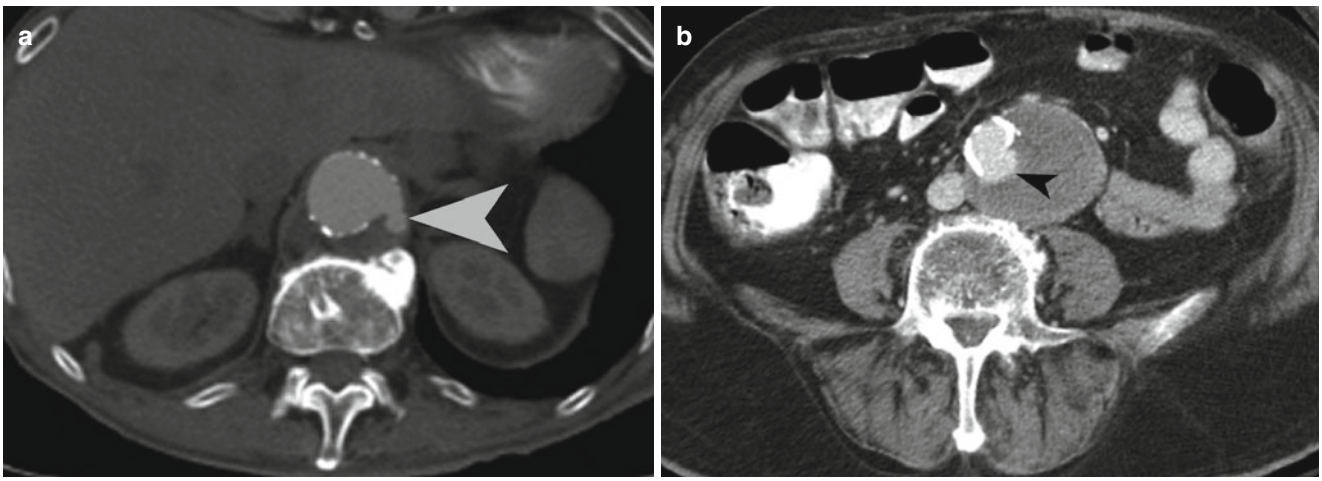

Fig. 1.9 Aortic ulcer. (**a** and **b**) Contrast-enhanced CT scan study of the abdomen demonstrates abdominal aortic aneurysm with an aortic ulcer (*arrowheads*) along with intramural hemorrhage

References

1. Rakita D, Newatia A, Hines JJ, Siegel DN, Friedman B. Spectrum of CT findings in rupture and impending rupture of abdominal aortic aneurysms. Radiographics. 2007;27:497–507.
2. Schwartz SA, Taljanovic MS, Smyth S, O'Brien MJ, Rogers LF. CT findings of rupture, impending rupture, and contained rupture of aortic abdominal aneurysm. AJR Am J Roentgenol. 2007;188:W57–62.
3. Petasnick JP. Radiologic evaluation of aortic dissection. Radiology. 1991;180:297–305.
4. Fisher ER, Stern E, Godwin II JD, Otto C, Johnson JA. Acute aortic dissection: typical and atypical imaging. Radiographics. 1994;14:1263–71.
5. Lepage MA, Quint LE, Sonnad SS, Deeb M, Williams DM. Aortic dissection: CT features that distinguish true lumen from false lumen. AJR Am J Roentgenol. 2001;177:207–11.
6. Sawhney NS, DeMaria AN, Blanchard DG. Aortic intramural hematoma: an increasingly recognized and potentially fatal entity. Chest. 2001;120:1340–6.
7. Hayashi H, Matsuoka Y, Sakamoto I, Sueyoshi E, Okimoto T, Hayashi K, et al. Penetrating atherosclerotic ulcer of the aorta: imaging features and disease concept. Radiographics. 2000;20:995–1005.
8. Sebastià C, Pallisa E, Quiroga S, Alvarez-Castells A, Dominguez R, Evangelista A. Aortic dissection: diagnosis and follow-up with helical CT. Radiographics. 1999;19:45–60.

Emergencies of the Biliary Tract

2

Caterina Missiroli and Ajay Singh

Gallbladder is seen as an anechoic structure with wall thickness of less than 3 mm on ultrasound imaging. The normal common bile duct caliber is up to 5 mm in young adults, and it progressively increases with age, at the rate of 1 mm for each decade above 40 years. The intrahepatic ducts should not be more than 2 mm in diameter (not more than 40 % of the caliber of the accompanying portal vein branch).

Gallstones are seen in up to 10 % of the population, most commonly in middle-aged and elderly females. While majority of gallstones have cholesterol as the main component, a minority of stones are constituted by calcium bilirubinate and are called pigment stones. Ten to twenty percent of the gallstones contain enough calcium to be visible on plain radiograph (Fig. 2.1a). The stones are most commonly multiple and sometimes faceted. A triradiate collection of nitrogen gas within the fissures inside the gallstone produces Mercedes-Benz sign (Fig. 2.1b and c).

Typically, gallstones are seen as echogenic foci with clean distal acoustic shadowing (Fig. 2.1d). *Wall echo shadow sign* refers to the parallel echogenic lines produced by a combination of the gallbladder wall, echogenic stone, and associated distal acoustic shadowing (Fig. 2.1e). The hypoechoic line seen between the two echogenic lines represents interposed bile. This sign is seen in gallbladder filled with either a single large gallstone or multiple small gallstones. Ultrasound has higher sensitivity than CT in diagnosing gallstones and is therefore the screening modality of choice. Although ultrasound remains the exam of choice for suspected cholecystitis, there are ever more cases of acute cholecystitis being detected today with CT in the evaluation of abdominal pain than in the past.

Majority of the patients with gallstones are asymptomatic. Sometimes the gallstone can cause transient gallbladder outflow obstruction, leading to biliary colic. Biliary colic patients present with transient pain for 1–3 h with nausea and vomiting. The symptoms subside when the gallstone falls back into the gallbladder or passes distally into the biliary tree.

Acute Cholecystitis

Acute cholecystitis usually is caused by the gallstone obstruction of the cystic duct or the gallbladder neck (one-third of cases). Acute cholecystitis without stones (5–10 % of cases) can be seen in patients with adenomyomatosis, gallbladder polyp, and malignant neoplasm [1, 2]. The predisposing factors for acute acalculous cholecystitis include history of trauma, mechanical ventilation, hyperalimentation, postoperative/postpartum state, diabetes mellitus, vascular insufficiency, prolonged fasting, and burns [2].

The clinical presentation includes right upper quadrant pain for more than 6 h (vs. biliary colic), nausea, vomiting, and fever in a patient with history of gallstones. No clinical or lab finding provides high enough positive predictive value in making the diagnosis of acute cholecystitis.

Imaging

Ultrasound is the first-line imaging modality in diagnosing acute cholecystitis because of wide availability, ability to detect gallstones as well as biliary ducts, and accuracy in diagnosing acute cholecystitis. The ultrasound findings of acute cholecystitis include gallbladder wall thickening (>3 mm), gallbladder distension (>5 cm transverse dimension), and positive Murphy's sign (Fig. 2.2) [1, 3]. Sonographic Murphy's sign by itself does not have a high

C. Missiroli, MD
Department of Diagnostic Imaging,
Azienda Ospedaliera della Provincia di
Lecco – Presidio Ospedaliero A. Manzoni, Lecco, Italy

A. Singh, MD (✉)
Department of Radiology,
Massachusetts General Hospital, Harvard Medical School,
10 Museum Way, # 524, Boston, MA 02141, USA
e-mail: asingh1@partners.org

A. Singh (ed.), *Emergency Radiology*,
DOI 10.1007/978-1-4419-9592-6_2,

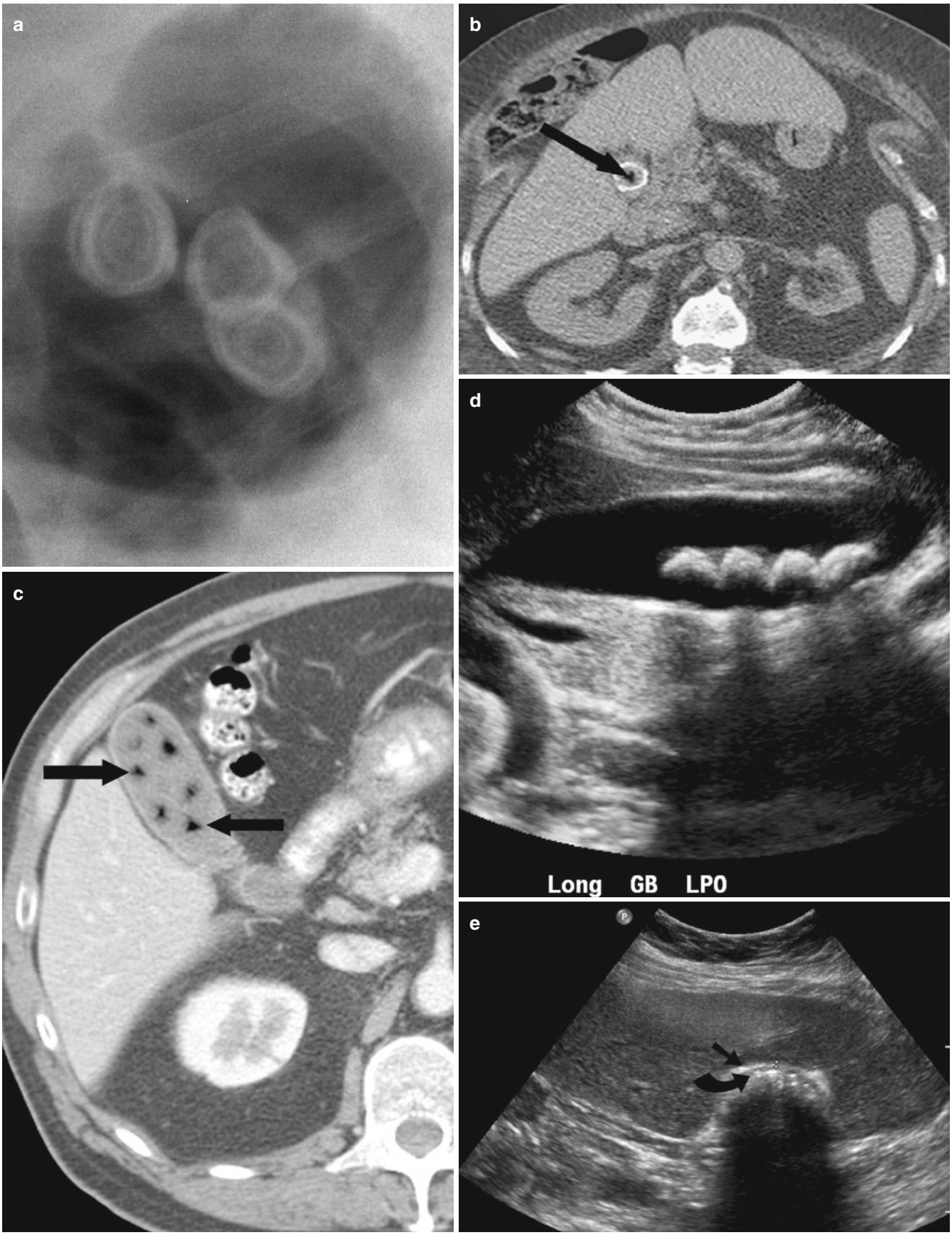
a
b
c
d
Long GB LPO
e

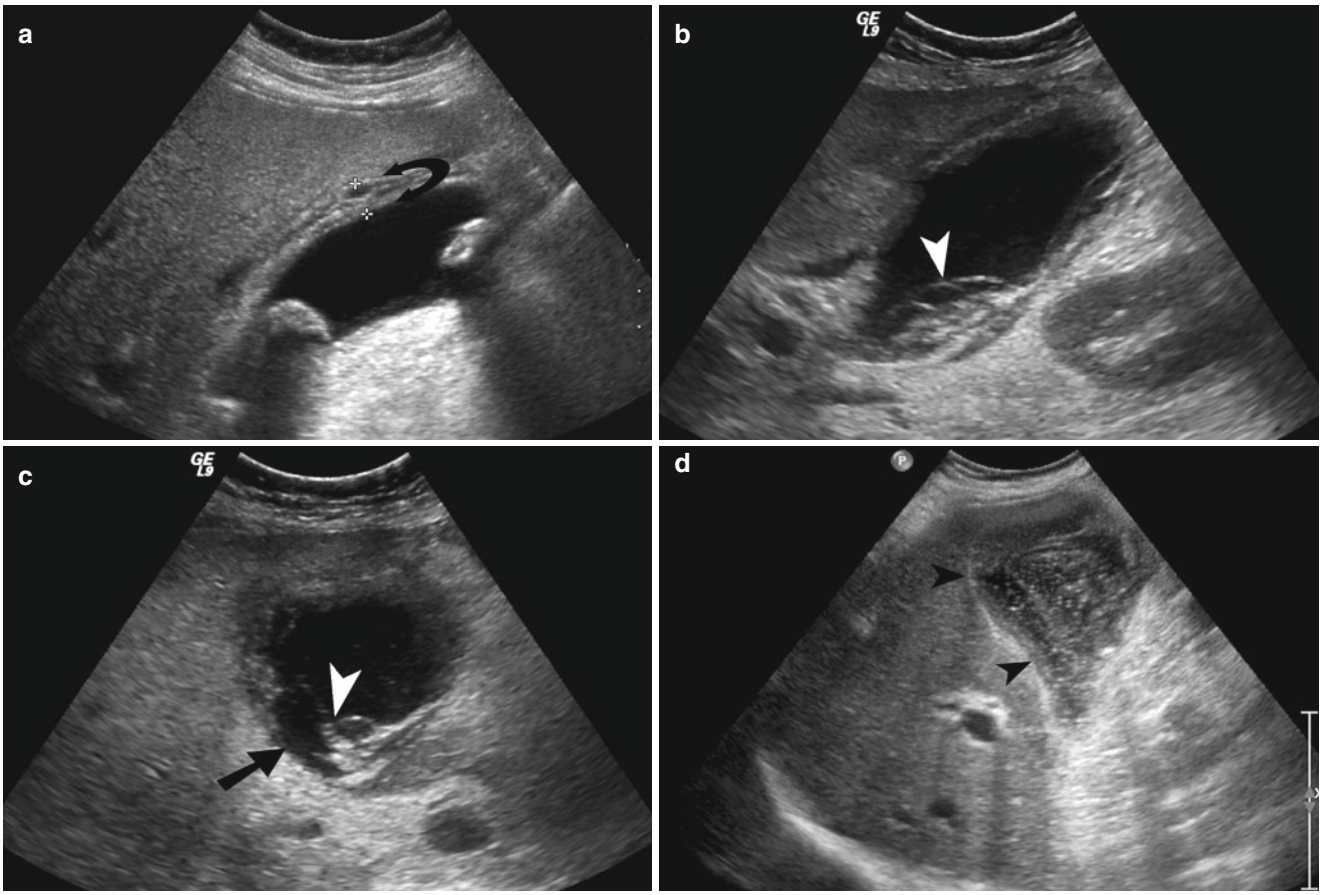

Fig. 2.2 Ultrasound imaging of acute cholecystitis. (**a**) Ultrasound in a patient with acute cholecystitis demonstrates multiple gallstones and striated thickening of the gallbladder wall (*arrow*). (**b** and **c**) Ultrasound in a patient with gangrenous cholecystitis demonstrates striated thickening of the gallbladder wall, intraluminal sludge, and sloughed mucosa (*arrowhead*). Focal thinning of the necrotic gallbladder is indicated by the *straight arrow* and appears to represent the donor site for the sloughed-off mucosa. (**d**) Ultrasound in a patient with acute cholecystitis shows gallbladder wall thickening (*arrowheads*) and complex fluid, which represented pus during cholecystostomy tube placement

positive predictive value and can be falsely negative in patients who have received analgesic medication. Another imaging finding of acute cholecystitis is the presence of a pericholecystic fluid collection, sometimes extending to the perihepatic space [2, 4].

Gallbladder wall thickening is a finding of acute cholecystitis which can also be seen in other conditions such as hypoproteinemia, ascites, pancreatitis, right heart failure, renal failure, liver failure, and hepatitis. Striated gallbladder wall thickening is no more specific for acute cholecystitis than the observation of gallbladder wall thickening from other causes. In the clinical setting of acute cholecystitis, the presence of striated gallbladder wall thickening suggests gangrenous cholecystitis.

Cholescintigraphy (HIDA scan) is considered second-line imaging modality which can be used after equivocal ultrasound study. Cholescintigraphy has a sensitivity and specificity which is superior to ultrasound. Although it may take more than 2 h to complete the study, the use of morphine (0.04 mg/kg) allows cholescintigraphy to be completed in 1.5 h. The classic findings on cholescintigraphy include nonvisualization of the gallbladder 30 min after morphine injection and presence of a curvilinear area of increased

Fig. 2.1 Imaging appearance of gallstones on plain radiograph and ultrasound. (**a**) Plain radiograph demonstrates laminated radiopaque gallstones in the *right upper quadrant*. Up to a fifth of the gallstones can be seen on plain radiograph of the abdomen. (**b** and **c**) Noncontrast CT of the gallbladder shows gallstones with Mercedes-Benz sign (*arrows*). Mercedes-Benz sign is due to nitrogen collection in triradiate configuration, within fissures of a gallstone. (**d**) Ultrasound shows multiple echogenic gallstones with distal acoustic shadowing, within the gallbladder lumen. (**e**) Ultrasound shows wall echo shadow sign in a patient with multiple gallstones and chronic cholecystitis. The outer echogenic line (*straight arrow*) represents the gallbladder wall, while the inner echogenic line (*curved arrow*) represents the outer edge of gallstones

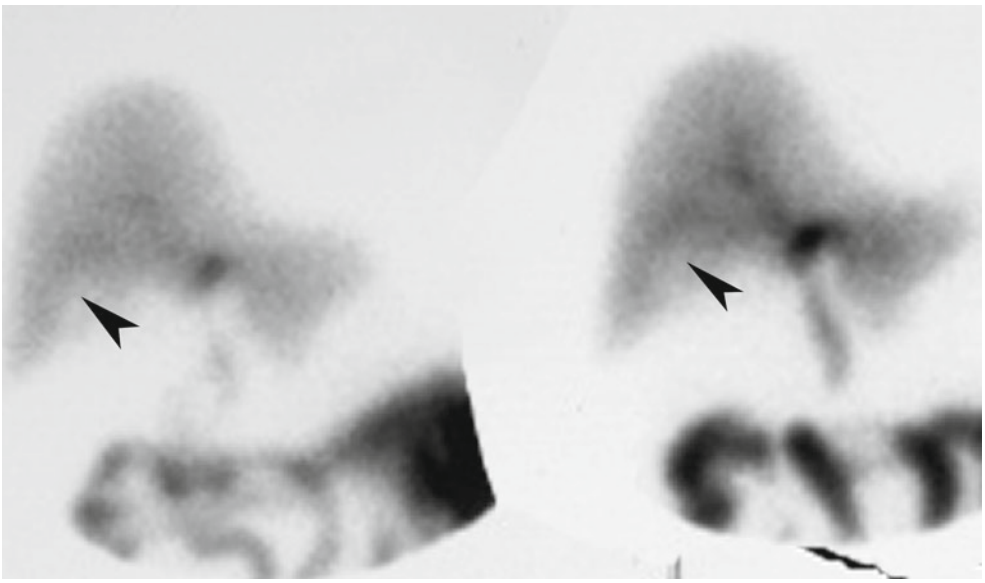

Fig. 2.3 Gangrenous cholecystitis on cholescintigraphy. Cholescintigraphy study (HIDA scan) demonstrates nonvisualization of the gallbladder and a curvilinear area of increased radiotracer activity (*rim sign*) in the pericholecystitic liver parenchyma (*arrowheads*)

radiotracer activity (rim sign) in the liver adjacent to the gallbladder (Fig. 2.3). Rim sign is most commonly seen in patients with gangrenous cholecystitis and is due to extension of inflammation beyond the gallbladder.

If ultrasound and/or cholescintigraphy show no evidence of acute cholecystitis or any other cause for the right upper quadrant pain, a contrast-enhanced CT is considered the next most appropriate imaging modality. The CT findings include gallstones, gallbladder wall thickening, gallbladder wall enhancement, increased bile attenuation (possibly indicative to empyema), distended gallbladder, and pericholecystic fluid collection (Table 2.1; Fig. 2.4) [5]. CT has lower sensitivity than US in detecting gallstones and can miss noncalcified gallstones.

Table 2.1 CT findings of acute cholecystitis

Thickening of the gallbladder wall (normal wall thickness is up to 3–4 mm)
Gallstones
Gallbladder distention (>5 cm in transverse dimension)
Pericholecystic fluid
Indistinct interface between the gallbladder wall and the liver
Pericholecystic inflammatory changes
Transient focal attenuation difference
Increased density bile

MR imaging is not a frontline imaging modality for acute cholecystitis and can be used after equivocal US study. The advantage of MR over CT is its ability to reliably study

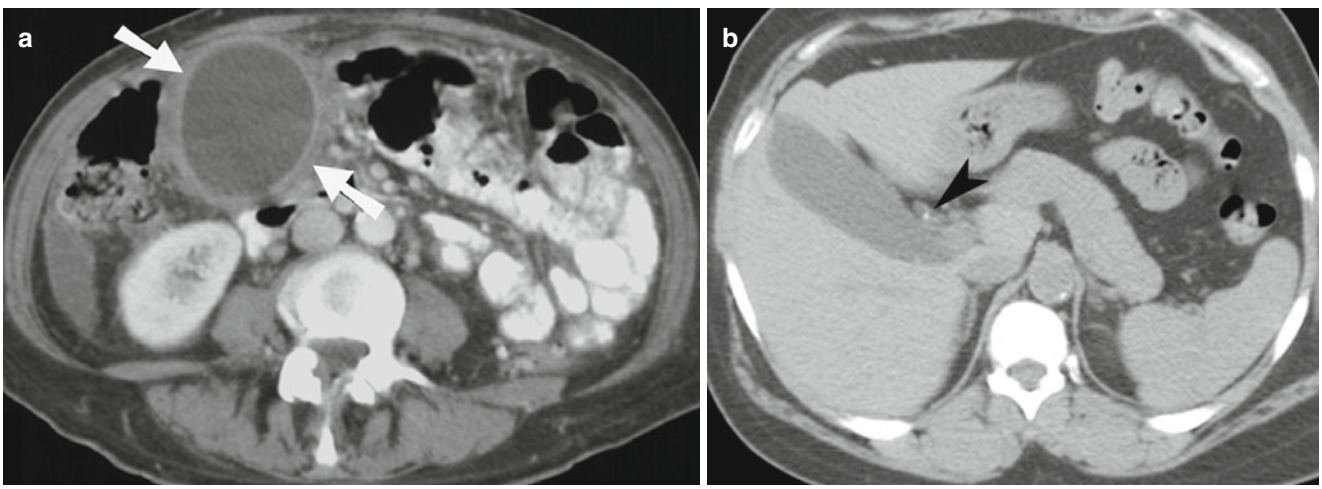

Fig. 2.4 CT findings of acute cholecystitis. (**a**) Contrast-enhanced CT shows distended gallbladder with wall thickening (*arrows*) and pericholecystic inflammatory changes. (**b**) Contrast-enhanced CT shows small calculus (*arrowhead*) causing cystic duct obstruction

common bile duct and the lack of ionizing radiation which is especially important in pregnant population. Although, gadolinium is useful in making the diagnosis of acute cholecystitis, it should not be used in pregnant population. The important findings of cholecystitis on MR imaging are described in Table 2.2 (Fig. 2.5).

The complications of acute cholecystitis include gallbladder empyema, gangrenous cholecystitis, emphysematous cholecystitis, gallbladder perforation, Mirizzi syndrome, and gallstone ileus.

Mirizzi Syndrome

The obstruction of the common bile duct or common hepatic duct by calculus impacted in the Hartmann's pouch or cystic duct constitutes Mirizzi syndrome (Fig. 2.6). Mirizzi syndrome or choledocholithiases should be suspected whenever there is elevated bilirubin level along with clinical symptoms of acute cholecystitis.

Table 2.2 MR findings of acute cholecystitis

Gallbladder empyema	Low-signal intensity on T2 and high-signal intensity on T1 WI
Gallstones	Signal void on MRCP and low signal on T1–T2 WI
Gallbladder wall thickening	Enhancing wall and high signal on T1 and low to high on T2 WI
Gas within the gallbladder wall	Signal void in the wall
Pericholecystic inflammation	High intensity on T1 and T2 WI
Hemorrhage	High intensity on T1 and T2 WI
Fluid collection	High intensity on T1 and T2 WI

Empyema

It is also called suppurative cholecystitis and occurs typically in diabetic patients, when the bile becomes infected and pus fills the distended gallbladder [1]. On imaging, gallbladder empyema is manifested as gallbladder distension, wall thickening, pericholecystic fluid accumulation, intraluminal sludge/pus, and intraluminal air (Fig. 2.7).

Gangrenous Cholecystitis

It is an advanced form of acute cholecystitis, most frequently seen in elderly men. It is characterized by increased intraluminal pressure, gallbladder distension, gallbladder wall necrosis, intramural hemorrhage, and abscess formation (Fig. 2.8) [1, 2]. There is an increased association of gangrenous cholecystitis with cardiovascular disease and leukocytosis of more than 17,000 WBC/mL. Although CT is highly specific (>90 %) in identifying patients with acute gangrenous cholecystitis, it is not very sensitive (Table 2.3).

Once gangrenous cholecystitis is suspected, the patients require emergency cholecystectomy or cholecystostomy to avoid life-threatening complications. These patients frequently require an open surgical procedure rather than laparoscopic cholecystectomy.

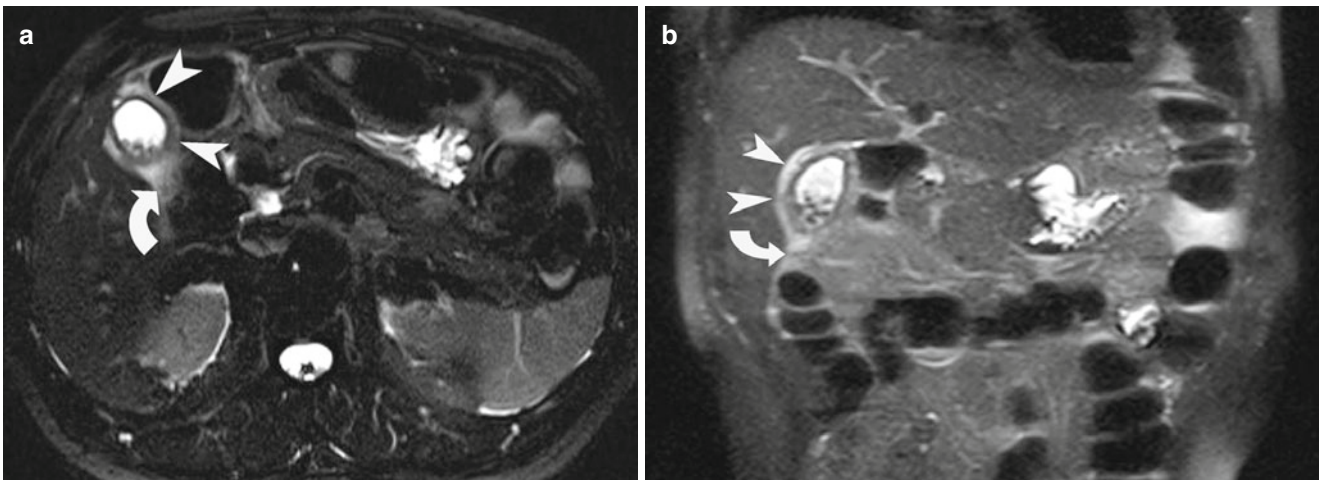

Fig. 2.5 MR findings of acute cholecystitis. (**a** and **b**) HASTE sequence shows gallbladder wall thickening (*arrowheads*), increased signal intensity (*curved arrows*), and multiple small gallstones. HASTE is a high-speed, heavily T2-weighted sequence with partial Fourier technique which has high sensitivity for fluid and a fast acquisition time (<1 s/slice)